

RL-TR-93-145
Final Technical Report
July 1993

AD-A270 949



(2)

EVALUATION OF LASER DIODE BASED OPTICAL SWITCHES FOR OPTICAL PROCESSORS

Cornell University

Paul D. Swanson (Cornell University),
Michael A. Parker and Stuart I. Libby (Rome Laboratory)

APPROVED FOR PUBLIC RELEASE; DISTRIBUTION UNLIMITED.

93-24740


DTIC
ELECTE
OCT. 20. 1993
S B D

Rome Laboratory
Air Force Materiel Command
Griffiss Air Force Base, New York


93 10 18 038

This report has been reviewed by the Rome Laboratory Public Affairs Office (PA) and is releasable to the National Technical Information Service (NTIS). At NTIS it will be releasable to the general public, including foreign nations. RL-TR-93-145 has been reviewed and is approved for publication.

APPROVED:


MICHAEL A. PARKER
Project Engineer

FOR THE COMMANDER:


DONALD W. HANSON
Director
Surveillance and Photonics Directorate

If your address has changed or if you wish to be removed from the Rome Laboratory mailing list, or if the addressee is no longer employed by your organization, please notify RL (OCPB) Griffiss AFB NY 13441. This will assist us in maintaining a current mailing list.

Do not return copies of this report unless contractual obligations or notices on a specific document require that it be returned.

REPORT DOCUMENTATION PAGE

Form Approved
OMB No. 0704-0188

Public reporting burden for this collection of information is estimated to average 1 hour per response, including the time for reviewing instructions, searching existing data sources, gathering and maintaining the data needed, and completing and reviewing the collection of information. Send comments regarding this burden estimate or any other aspect of this collection of information, including suggestions for reducing this burden, to Washington Headquarters Services, Directorate for Information Operations and Reports, 1215 Jefferson Davis Highway, Suite 1204, Arlington, VA 22202-4302, and to the Office of Management and Budget, Paperwork Reduction Project (0704-0188), Washington, DC 20503.

1. AGENCY USE ONLY (Leave Blank)		2. REPORT DATE July 1993		3. REPORT TYPE AND DATES COVERED Final Mar 92 - Dec 92	
4. TITLE AND SUBTITLE EVALUATION OF LASER DIODE BASED OPTICAL SWITCHES FOR OPTICAL PROCESSORS				5. FUNDING NUMBERS C - F30602-92-C-0038 PE - 62702F PR - 4600 TA - P3 WU - PF	
6. AUTHOR(S) Paul D. Swanson, Cornell University Michael A. Parker, Stuart I. Libby, Rome Laboratory					
7. PERFORMING ORGANIZATION NAME(S) AND ADDRESS(ES) Cornell University Office of Sponsored Programs 123 Day Hall Ithaca NY 14853-2801				8. PERFORMING ORGANIZATION REPORT NUMBER	
9. SPONSORING/MONITORING AGENCY NAME(S) AND ADDRESS(ES) Rome Laboratory/OCPB 25 Electronic Parkway Griffiss AFB NY 13441-4515				10. SPONSORING/MONITORING AGENCY REPORT NUMBER RL-TR-93-145	
11. SUPPLEMENTARY NOTES Rome Laboratory Project Engineer: Michael A. Parker/OCPB/(315)330-7671.					
12a. DISTRIBUTION/AVAILABILITY STATEMENT Approved for public release; distribution unlimited.				12b. DISTRIBUTION CODE	
13. ABSTRACT (Maximum 200 words) Three optical switching elements have been designed, fabricated and tested for use in an integrated, optical signal processor. The first, an optical NOR logic gate uses gain quenching as a means of allowing one (or more) light beam(s) to control the output light. This technique, along with the use of a two pad bistable output laser, is used in demonstrating the feasibility of the second device, an all optical RS flip flop. The third device consists of a broad area orthogonal mode switching laser, whose corollary outputs correspond to the sign of the voltage difference between its two high impedance electrical inputs. This device also has possible memory applications if bistable mode switching within the broad area laser can be achieved.					
14. SUBJECT TERMS optical logic, optical memory, lasers				15. NUMBER OF PAGES 24	
				16. PRICE CODE	
17. SECURITY CLASSIFICATION OF REPORT UNCLASSIFIED	18. SECURITY CLASSIFICATION OF THIS PAGE UNCLASSIFIED	19. SECURITY CLASSIFICATION OF ABSTRACT UNCLASSIFIED	20. LIMITATION OF ABSTRACT U/I		

ACKNOWLEDGMENTS

The authors would like to acknowledge useful discussions with Prof. C. L. Tang, John Johnson, and G. Porkolab of Cornell University, along with J. Fitz of the National Security Agency. We would also like to thank the personnel of the National Nanofabrication Facility at Cornell University for their technical support.

M. A. Parker and P. D. Swanson designed and fabricated the optical switches. S. I. Libby assisted with the characterization of the devices.

DTIC REPORT NUMBER 8

Accession For	
NTIS	<input checked="" type="checkbox"/>
DEPT. OF	<input type="checkbox"/>
UNIVERSITY	<input type="checkbox"/>
GOVERNMENT	
P	
1000	
Available for 6 days	
Dist	
A-1	

I. INTRODUCTION

The expanding use of optical signals to transfer data makes all optical signal processing desirable.¹ The thrust of this research has been to investigate the feasibility of using laser diode based in-plane optical switches as the building blocks for an optical processor. Such switching devices include optical logic gates and memory elements, as well as electrically controlled optical switches. The output of all the devices studied was provided by a semiconductor laser diode, while the on and off states of the laser diode was based on whether or not the round trip optical gain in the laser exceeded the round trip optical loss. External optical and/or electrical input controlled the gain and loss by means of optical gain quenching and/or optical saturation.²⁻⁷ Memory elements require that the output laser be able to maintain two levels of output for the same biasing conditions (bistability). This was achieved by having the output laser cavity loss dependent on the cavity's internal optical intensity. Three switching devices were evaluated: an optical NOR gate; an optical RS flip flop; and a broad area orthogonal mode switching laser. All of the devices were fabricated from Graded Index Separate Confinement Heterostructure (GRINSCH) GaAs-AlGaAs Multiple Quantum Well wafers, as shown in Figure 1.

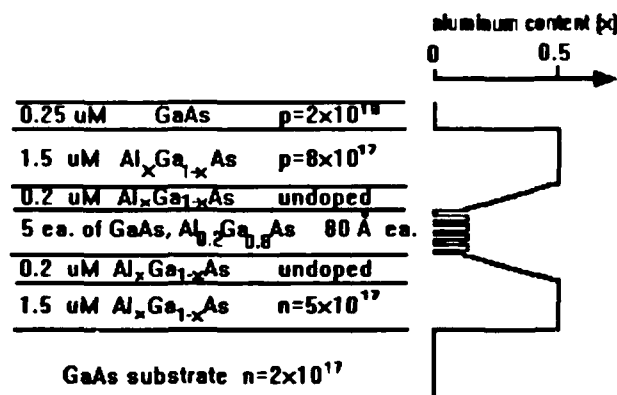


Figure 1: The grown epitaxial laser structure used for all of the devices in this study.

In the sections that follow, the theoretical and measured performance of each of the switches is presented.

II. NOR LOGIC GATE

All Boolean logic can be performed with a combination of NOR gates. Figure 2 shows the optical NOR gate designed, fabricated, and tested for this study. The gate consists of three GaAs-AlGaAs heterostructure lasers operating at a wavelength of 860 nm. The main laser can be quenched off by either of the two side lasers for the NOR operation. Quenching occurs when light perpendicular to the main laser cavity is amplified by the main laser's gain medium. Since the perpendicular gain is no longer available to amplify light traveling in the main laser, the round trip gain of the main laser decreases. If the round trip gain falls below the round trip loss, then the main laser will turn off. The main laser can be turned off by either a perpendicular laser intersecting its cavity or by an intersecting optical amplifier coupled to an external optical input. For the purpose of this study intersecting laser cavities were used. The design shown in Figure 2 improves upon previous designs by using hole coupled total internal reflection mirrors to control the internal loss/gain ratio while minimizing laser threshold currents.⁶⁻⁷

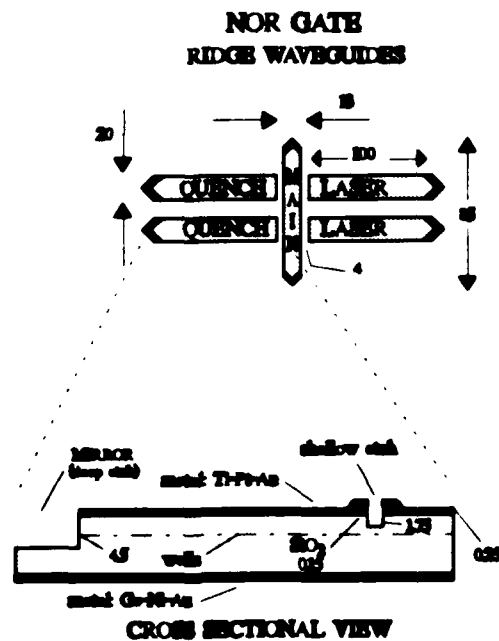


Figure 2: The etched ridge waveguide NOR gate, top view and partial side view.¹⁴

L-I curves of the main laser in the NOR gates were taken in order to determine threshold currents and relative mirror reflectivity. The experimental setup for obtaining the L-I curves appears in the inset to Figure 3. The pulse generator produced 5 μ sec wide pulses separated by 2 msec. The pulse itself was the positive portion of a sine wave. It was applied to the series combination of the main laser and a 50 Ω current sampling resistor which were joined at the bottom N⁺ contact. This resistor yielded a voltage drop proportional to the current through the laser. A single mode fiber, with one end positioned next to a facet of the main laser, routed the illumination to a PIN photo diode circuit. A digital oscilloscope plotted the pin diode signal versus the signal across the 50 Ω resistor.

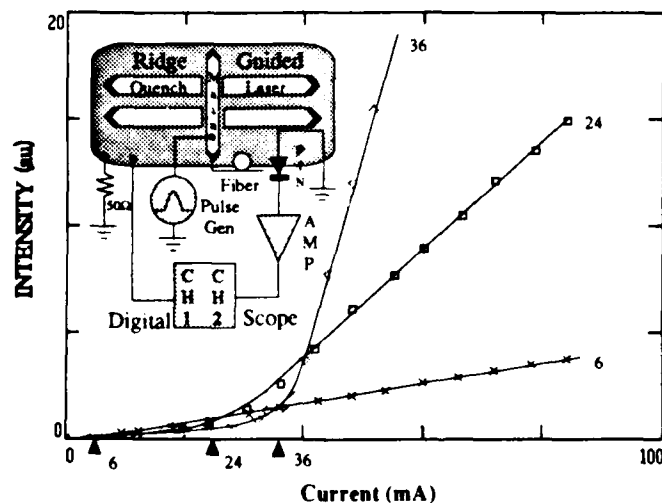


Figure 3: The L-I curves from main lasers with TIR mirrors in three different NOR gates. The numbers next to the triangles indicate the threshold currents. The inset shows the device and the experimental arrangement.

The L-I curves for three different main lasers with TIR mirrors and etched ridge waveguides appear in Figure 3. Thresholds of 6, 24, and 36 mA were observed. The variation in threshold current and differential efficiency for the three devices stems from the variation in rounding of the tip of the roof shaped TIR mirrors. The rounded tips acted as hole couplers of varying aperture size; the lasers with the lower threshold current and differential efficiency had smaller apertures, and therefore greater mirror reflection.¹⁸

The quench experiments were conducted with the apparatus depicted by the block diagram in the inset to Figure 4. A pulse generator applied a voltage to the main laser for about 10 microseconds. During this time, a second synchronized pulse generator drove the side laser with a triangular wave of the same duration as the pulse in the main laser. One end of an optical fiber probed the emitted light. A pin photo diode and amplifier detected and amplified the optical signal and then applied the resulting signal to the digital oscilloscope. The currents through the main and side lasers were determined by monitoring the voltage across $10\ \Omega$ resistors in series with the pulse generators (not shown).

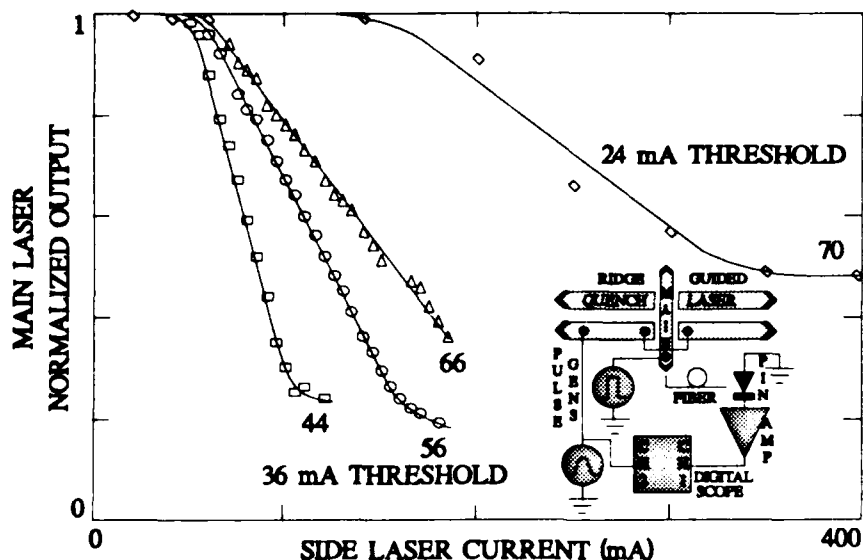


Figure 4: Normalized irradiance from the main lasers of two NOR gates as a function of the current into the side lasers; threshold currents of 36 and 24 mA were determined from Figure 3 for these lasers. The quenching effect was observed for the 36 mA NOR gate with 44, 56 and 66 mA into the main laser and for the 24 mA NOR gate with 70 mA into the main laser.

Measured quenching data for the devices tested appear in Figure 4. The graph plots the emitted power from the main laser as a function of the current injected into the side laser. The unquenched output power of each device was normalized to unity. The first three curves correspond to the device with the 36 mA threshold current for the main laser while the right most curve corresponds to the device with the 24 mA threshold current. The irradiance from the 6 mA device was too small for accurate measurements. The curves are labeled with the value of their corresponding main laser driving current.

Approximately 80% of the optical power from the main laser can be quenched. Note the fairly linear decrease in main laser intensity as the side laser current increases. Also note that more side laser current is required for larger main laser currents in order to maintain a constant amount of quench. The gate with the 24 mA threshold for the main laser required larger quench currents than the gate with the 36 mA threshold for the main laser; in addition, this main laser could be quenched by no more than 50%.

The quenching can not be attributed to electrical crosstalk between the metal pads on the P^+ surface of the wafer. Both the main and side lasers must be electrically biased in the same way.¹⁵ Therefore, electrical crosstalk would cause the current in one laser to increase as the current in the others increase. If this was the case, the power emitted from the main laser would increase with increasing side laser power. Any resistance in the N^- layer or in the circuit connecting the metal on the N^- layer on the bottom of the wafer could give rise to curves which resemble the quench curves of Figure 4, however, based on the doping level, the thickness of the N^- layer,¹⁷ and the device sizes, the typical resistance in this layer is on the order of 0.1Ω . Any voltage drop across this resistance would be relatively small and could not account for the quench data, and therefore, the quenching shown in Figure 4 is in all likelihood due to true gain quenching.

The gain quenching curves in Figure 4 can be divided into three regions; the spontaneous emission region (SPR), the linear region (LR), and the side laser saturation region (SR). The SPR corresponds to side laser currents smaller than ~ 50 mA. This corresponds to when the side laser is below its threshold current, and thus no coherent light intersects the main cavity. This would be similar to an intersecting optical amplifier with zero input. In either case zero input yields a high output on the main laser. In the LR region, where the side laser is beginning to lase, the irradiance from main laser linearly decreases. This linear decrease occurs as a result of the probabilistic nature of the interaction between light and the electron-hole transitions in the common gain region. A photon from either the side or main laser can stimulate the emission of a photon in such a way that the wave vector of this emission is parallel to either the quench or main laser cavity respectively. The photon density in the side laser is linearly proportional to the side laser pump current for currents above threshold and below saturation. Thus the probability of

interaction between photons from the side laser and electron-hole pairs in the common cavity increases linearly. As the side laser current increases, the common cavity region produces more photons with wave vectors parallel to the side laser and less with wave vectors parallel to the main laser. The main laser loses the contribution of the common cavity to its gain, with the loss being linear to side laser current. Thus the main laser output decreases linearly in the LR. The SR occurs either when the gain in the side laser saturates or when the common gain region is fully quenched. The intensity at which the output of the main laser saturates can be lowered by either increasing the length of the side laser (or amplifier) or by increasing the percentage of the main laser gain region which is intersected by the side laser. This minimum intensity of the main laser defines the "zero" output state of the logic gate.

III. RS FLIP FLOP

If the main laser of the NOR gate described in the previous section is made bistable by the means of an intensity dependent saturable absorber, the resulting device would be an optical RS flip flop. The side laser would reset the main laser to the zero state, while a high intensity beam coupled into the main laser itself would set it back to the high state.¹⁶ This flip-flop can be divided into 3 functional blocks (refer to Figure 5). (1) A main laser cavity contains *gain* and *saturable absorber* sections²⁻⁵ which induce bistable output characteristics; this functional block provides the logical 0 or 1 state. (2) An external laser *pumps* the saturable absorber and *sets* the output to the logic 1. (3) A second external laser *quenches*^{6,7} the main laser and *resets* the output to the logic 0. Both setting and resetting lasers (2 & 3) could be replaced by optical amplifiers coupled to external optical inputs. As with the NOR gate, these lasers are monolithically integrated on AlGaAs-GaAs quantum well heterostructure; emitting at 860 nm. The main cavity has one Total Internal Reflection (TIR) mirror⁷ and a flat etched mirror which separates it from the pump laser. Reflections can occur at the discontinuity in the index of refraction accompanying the electrical isolation between the pumped and unpumped regions; thus the cut across the electrode is angled to inhibit the formation of a shorter cavity within the main cavity. The quench laser is divided into two parts across the gain region of the main laser⁷ so that the quench and main laser

cavities overlap; the two halves of the quench laser are electrically connected in parallel. All four gain sections are optically confined, but the voltage controlled saturable absorber is unguided.

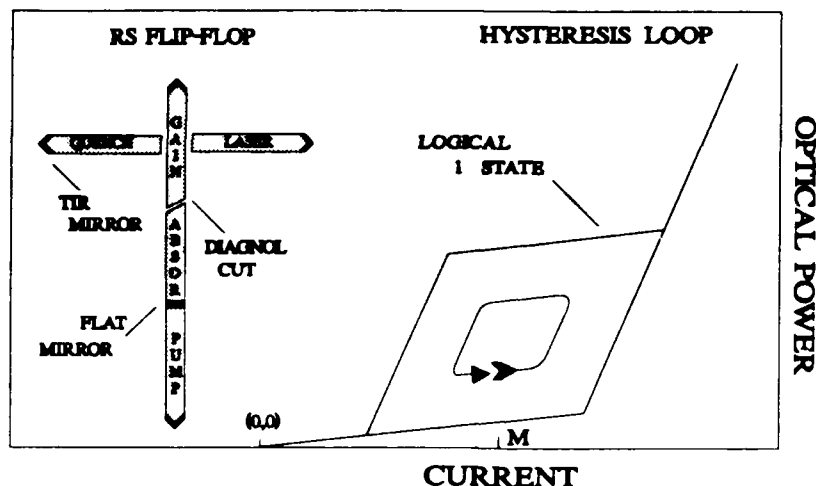


Figure 5: The RS flip flop and the desired hysteresis in the L-I characteristics. Scale: the gain section is on the order of $5 \times 100 \mu\text{m}$.

The operation of the flip-flop depends on the ability of the pump and quench laser to set and reset the output state of the main cavity respectively. Figure 5 also shows a qualitative plot of the intensity of the light emitted from the main laser versus the current into the gain section. The current in the main laser gain section is adjusted to point M where the output intensity can be in either of two states. Assume that initially the output of the main laser corresponds to a point on the lower branch of the hysteresis loop. A momentary optical pulse from the pump laser bleaches the absorber, lowers the threshold current below point M and, therefore, sets the output to the upper branch of the hysteresis loop. The bistable nature of the gain-absorber pair ensures that the output will remain on the upper branch for times longer than the width of the pulse. When a momentary optical pulse from the quench laser stimulates emission in the common cavity, the wavevector of this stimulated emission is parallel to the cavity of the quench laser instead of the main laser. This process reduces gain in the main cavity, raises the lasing threshold current and, thereby, resets the output of the main laser to the lower branch of the hysteresis curve.

Since the device parameters required for gain quenching was already determined by the NOR gate study, the main thrust of the RS flip flop development was to optimize the hysteresis loop of the bistable main laser. The saturable absorber plays the key role in the bistability. It must induce the hysteresis loop shown in figure 5 and it must be capable of being bleached by illumination from a secondary laser in such a way that the main cavity begins to lase from an initially off state. The saturable absorber experiments include tests for (1) the hysteresis induced in the L-I curve of the main laser and (2) the width of the hysteresis loop as a function of the applied voltage.

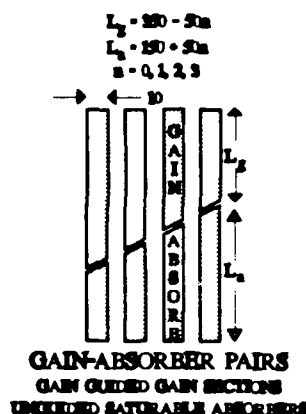


Figure 6: Main laser gain / saturable absorber pairs used to optimize output hysteresis as a function of internal optical density. The lasers were 350 microns long. The best results were achieved in devices with unguided saturable absorbers 150 microns long.

In one series of experiments, ridge guided gain-absorber pairs were tested for hysteresis in the L-I characteristics. These pairs included those with (1) wet and CAIBE etched waveguides, (2) various lengths of gain and saturable absorber sections and (3) single and multimode waveguides. Hysteresis was not observed in any of the ridge guided devices. In another series of experiments, hysteresis was observed in devices with gain guided gain sections and unguided saturable absorbers; these devices are depicted in Figure 6.

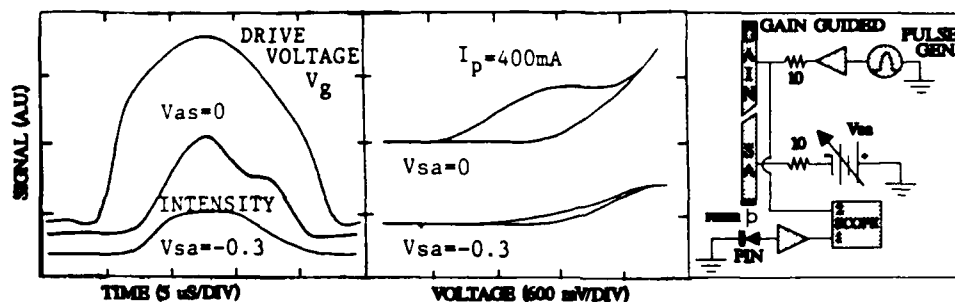


Figure 7: The left side shows plots of the timing relation between the drive voltage to the gain section of the gain-absorber pairs and the emitted irradiance from the pair; the irradiance is shown for two voltages on the saturable absorber. The middle panel shows the hysteresis loop for the emitted irradiance vs. drive voltage. The experimental setup is shown on the right. V_{sa} and I_p are the saturable absorber voltage and peak drive current for the gain section respectively.

The results for the optimized device appear in Figure 7. The vertical axis has arbitrary units in either voltage or irradiance. The left side of the plot shows the timing relation between the drive voltage to the gain section and the irradiance emitted through the saturable absorber. The hysteresis curves on the in the middle section are plots of the irradiance vs. the drive voltage. The two intensity plots correspond to two different voltages applied to the saturable absorber. The slight asymmetry of the drive voltage results from the I-V and L-I characteristics of the laser diode as can be seen by comparing the drive voltage curve to the intensity curves.

Of particular interest is the hump on the right side of the $V_{sa}=0$ intensity plot. Once the saturable absorber is bleached, it remains in that state for values of current into the gain section which are less than the initial threshold current. It is this hump which produces the upper hysteresis loop in Figure 7.

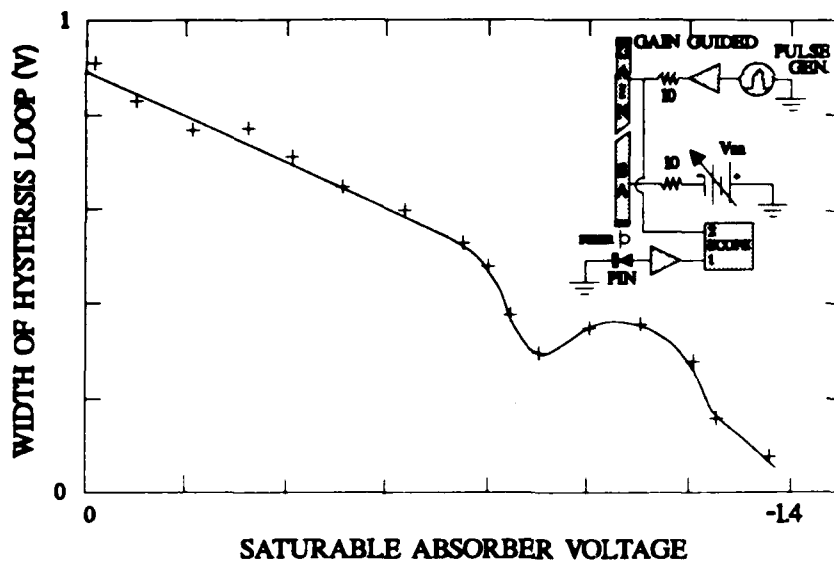


Figure 8: The width of the hysteresis loop as a function of the voltage applied to the saturable absorber. The effects of RC time delays have not been removed from the data which probably dominate the other effects in determining the width of the observed loops beyond about -0.6 volts. The inset shows the experimental setup used to observe the hysteresis loop.

Figures 7 and 8, shows that an increase of the reverse bias voltage causes the irradiance, the width and height of the loop to decrease. The loops can not be attributed to heating effects as the system would transverse the loop in a clockwise direction rather than the counter clockwise direction observed for these loops. In Figure 8, no attempt was made to correct for RC effects, which probably dominate beyond about -0.6 volts. In the optimum saturable absorber biasing region, between zero and -0.6 volts, RC effects are not dominant.

It was observed that the position of the single mode fiber strongly influenced the shape of the observed L-I curves. We attributed this behavior to multiple spatial modes in the laser displaying differing degrees of bistability.

Hysteresis in the optimized gain-absorber pairs can be attributed to optical saturation within the saturable absorber. The component of the round trip loss due to the saturable absorber decreases with increasing photon density. The photon density becomes orders of magnitudes larger when a laser's round

trip gain begins to exceed its round trip loss. This, in turn, reduces the round trip loss by saturating the absorber. Thus the laser will require a high photon density (large current) to turn on, yet will remain on if the photon density (pump current) is reduced below the initial value required. When the photon density decreases to the point that the saturable absorber is no longer saturated, the device will turn off. The voltage dependence of the loop width can be attributed to the quantum confined stark effect. The fact that the hysteresis was not observed for saturable absorbers with ridge waveguiding is most likely due to the guided spontaneous emission from the gain section saturating the absorber before the lasers reached threshold conditions. In this case loss due to the saturable absorber would be constant and no bistability would be observed. The gain guided structure greatly decreases the spontaneous emission entering the absorber section, and thus is less likely to saturate prematurely. Another possibility contributing factor could be intensity dependent self focusing of the light in a unguided saturable absorber due to spatial hole burning.¹⁹

Combining the results of Figure 7 with that of Figure 4 shows the feasibility of the use of saturable absorption and gain quenching to facilitate RS flip flop operation.

IV. BROAD AREA ORTHOGONAL MODE SWITCHING LASER

The third device, a Broad Area Orthogonal Mode Switching Laser (BAOMSL), shown in Figure 9, consists of a new single element, broad area, semiconductor laser with differential voltage control.⁸⁻¹⁰ With mirrors on all four sides, this laser can operate in orthogonal directions, each competing for the same gain.¹¹ Each of the two orthogonal cavities contains a saturable absorber which controls each cavities' round trip loss. Both cavities compete for the same gain; the cavity with the lowest internal loss will lase. A patterned SiO₂ layer under the gain section metallization delineates two orthogonally intersecting gain guided arrays (GGA), eliminating the possibility of circular modes. The gain section was 200 μm by 200 μm while each absorber section was 3 μm by 200 μm . The arrays consisted of two orthogonal sets of seven 15 μm wide guides on 25 μm centers. Shallow etches of 3 μm wide and 1.75 μm deep through the cap and cladding layers into the P⁺ GaAs provided electrical isolation between the modulators and the laser.¹⁴ The four mirrors were formed by deep etches of 4.5 μm .¹²⁻¹³

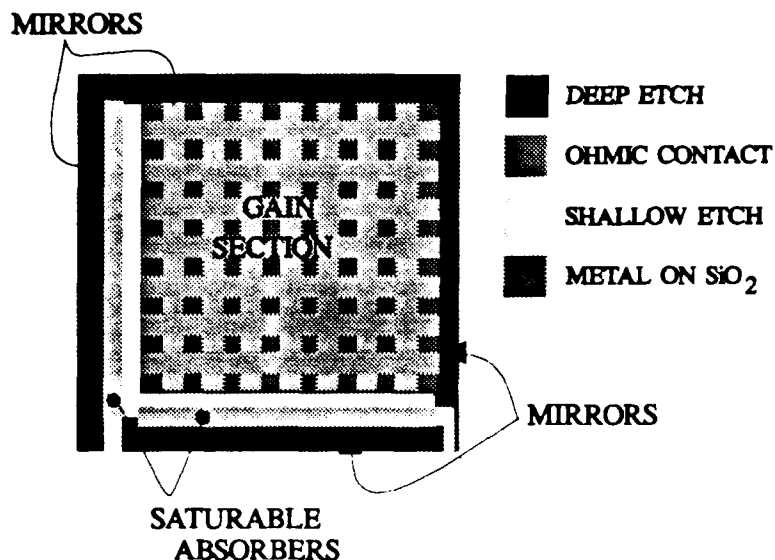


Figure 9. A broad area orthogonal mode switching laser incorporating a gain guided array capable of lasing in either of two orthogonal directions. The saturable absorbers control stimulated emission in the two directions. The four mirrors are formed by deep etches through the active region by Chemically Assisted Ion Beam Etching. Shallow etches into the top cladding layer provide electrical isolation between the saturable absorbers and the gain section. A patterned SiO_2 layer under the metallization allows for gain guiding. The gain section is $200\text{ }\mu\text{m}$ by $200\text{ }\mu\text{m}$.

The BAOMSL were tested for power output vs. pump current (L-I), the emission spectra, the intensity profile, the divergence angle, and the affect of absorber bias on the lasing state and the spectrum. L-I curves were obtained by cleaving one of the heterostructures through the deep etch, thereby exposing one of the facets. A fast, large area photo-detector was moved to within 0.5 cm of the laser facet. A series of low duty cycle triangular current pulses was applied to the lasers. The data was displayed as photo detector current vs. pump current on a digital oscilloscope. Optical emission spectra were obtained by angling an optical fiber with a $60\text{ }\mu\text{m}$ core just above the deep etch and within 10 to $20\text{ }\mu\text{m}$ of the laser facet. The drive current consisted of rectangular current pulses with the same temporal profile as those for the L-I curves. The spectrum of the light from the fiber was measured using an Anritsu optical spectrum analyzer set in an averaging mode. (3) The divergence angle was obtained by placing a CCD camera next to the laser with the cleave through the deep etch. After photographing the transverse mode pattern, the camera was displaced away from the laser by an additional 5 mm and the

pattern was again photographed. The separation of two lateral lobes was then compared between the two photographs to determine the divergence angle. The effect of absorber bias on the lasing state and spectra was obtained in a manner similar to that of the L-I curves.

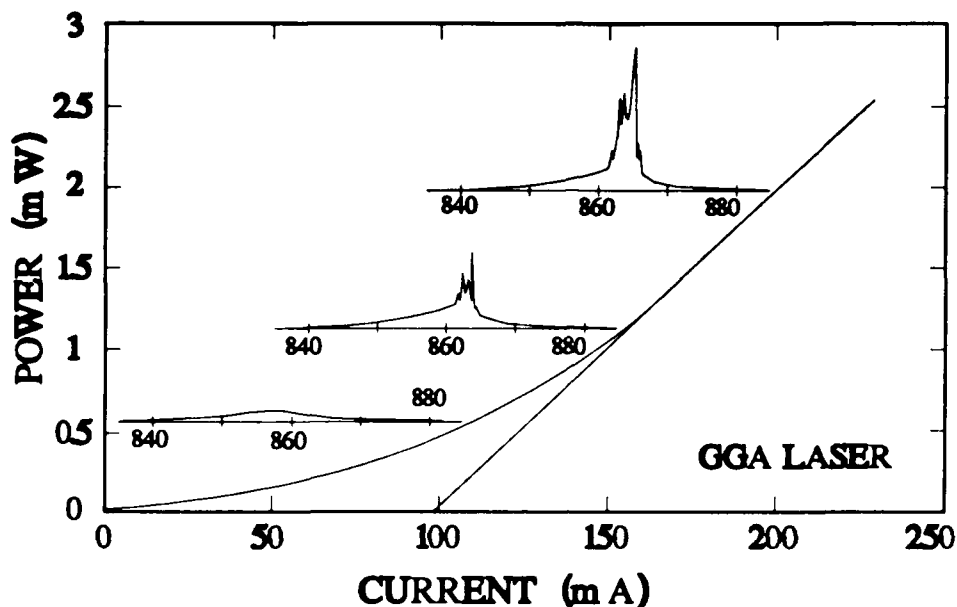


Figure 9: Emitted optical power versus drive current for the BAOMSL. The tangent line yields the extrapolated threshold current of 100 mA. The inset plots show the spectra at currents of 100, 150 and 200 mA.

Figure 9 shows the L-I curve for the GGA BAOMSL laser with both modulators grounded. The straight line portion of the graph yields a differential efficiency of 0.02 W/A and an extrapolated threshold current of 100 mA. The straight-line construction for extrapolating the threshold current is also shown in the figure. The inset graphs show the emission spectra for 100, 150 and 200 mA. The emission is entirely spontaneous at 100 mA. For 150 and 200 mA, the dominant lasing mode occurs near 865 nm. The far field pattern showed a transverse mode pattern consisting of many closely spaced nodal points diverging at an angle of 30 degrees.

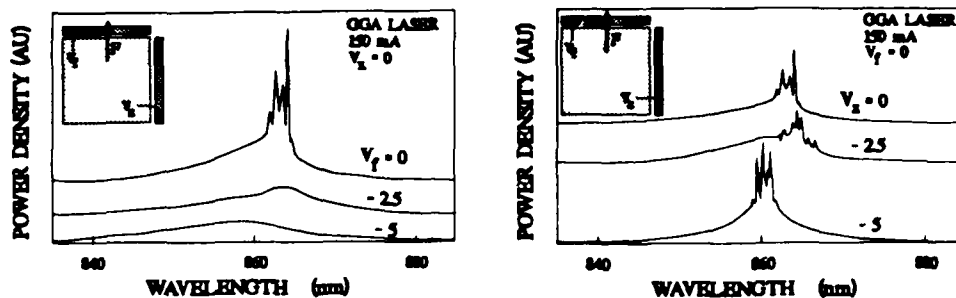


Figure 10: LEFT: Spectra for GGA laser emission through the saturable absorber with variable voltage V_f ; the other saturable absorber is grounded. Reverse biasing V_f cuts off laser oscillation. RIGHT: Spectra for GGA laser emission through the grounded saturable absorber; the voltage on the other saturable absorber varies. Reverse biasing V_x causes blue shifts in the spectrum and an increase in the peak intensity.

Figure 10 shows the emission spectra for the GGA BAOMSL with drive currents of 150 mA for various modulator bias voltages. Note that increasing the reverse bias voltage of either absorber section will make it harder for the device to lase in the direction transverse to the absorber and easier for the device to lase parallel to the absorber. Since both laser cavities are competing for the same gain, the cavity with the lower reverse bias transversing it will lase, while the cavity with the higher reverse bias will turn off. Thus this device acts as a differential voltage comparator with corollary output. If the absorbers could be made to saturate, as described in section III, this device could also be used as a memory element.

In order to show the importance of the gain guided array to the function of this device similar measurements were taken on a BAOMSL with the gain area uniformly pumped (UP). The results are shown on Figure 11. In contrast to the GGA laser, reverse bias applied to either modulator of the UP laser extinguishes all laser oscillation. This suggests that the two orthogonal cavities in the UP laser are strongly coupled and thus act as only one cavity.

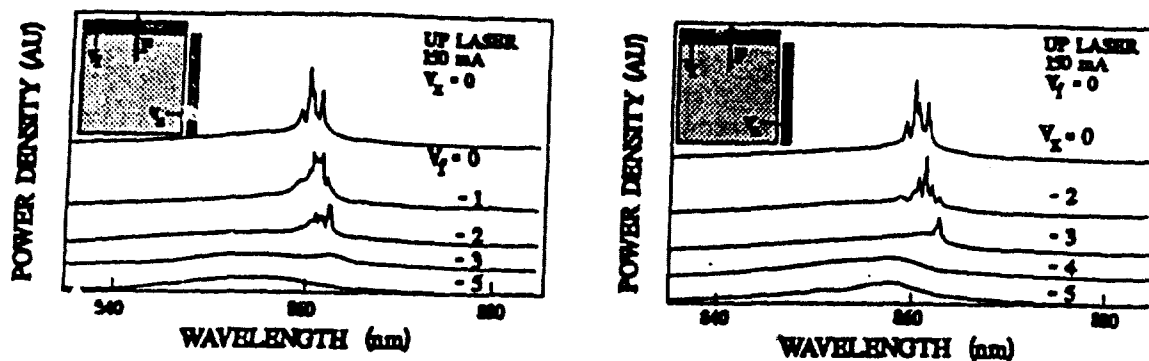


Figure 11: LEFT: Spectra for UP laser emission through the saturable absorber with variable voltage V_f ; the other saturable absorber is grounded. RIGHT: Spectra for UP laser emission through the grounded saturable absorber; the voltage on the other saturable absorber varies. The dominant mode for the UP laser is near 860 nm, compared to 865 nm for a GGA laser of similar dimensions.

V. DISCUSSION

These results show that optical switching based on controlling the net round trip gain/loss of a semiconductor laser is feasible for a wide array of applications. The practicality of integrating such switches into systems greatly depends on improving the quality of the devices. The measured performance of the individual devices reported on represents an ongoing effort in device optimization. Still, the operating currents presented may be impractical for large scale integration; electrical isolation still needs to be improved; and device yield and life time need to be addressed. These issues have driven an effort to improve basic device performance levels by means of improved device processing techniques. It is highly likely that these device parameters can be improved to acceptable limits, and therefore should not detract from the evaluation of the switching mechanisms in general.

VI. SUMMARY AND CONCLUSIONS

Three laser diode based optical switches were designed, fabricated, and tested. The first, a NOR gate, successfully demonstrated that a laser diode can be turned off by high intensity coherent light intersecting it. For the second device it was shown that if such a laser diode was made bistable, an optical RS flip flop could be fabricated. The third device, a broad area orthogonal mode switching laser, demonstrated that gain quenching could be used to fabricate a laser with two corollary outputs. The future of such devices depends on addressing the systems issues which hinder their ultimate practicality.

VII. REFERENCES

1. D. G. Fettielson, *Optical Computing*, MIT Press, Cambridge (1988)
2. G. J. Lasher, *Solid-State Electronics*, 7, 707 (1964)
3. T. Odagawa and S. Yamakashi, *Electronics Letters*, 25, 1429 (1989)
4. T. Ueno and R. Lang, *J. Appl. Phys.* 58, 1689 (1985)
5. C. Harder, K. Y. Lau, A. Yariv, *IEEE J. Quantum Electr.* QE-18, 1351 (1982)
6. W. J. Grande and C. L. Tang, *Appl. Phys. Lett.* 51, 1780 (1987)
7. W. Jung and Y. Kwon, *Jap. J. Appl. Phys.* 28, L1242 (1989)
8. M. A. Parker, S. I. Libby, A. J. Gerrald, P. D. Swanson, W. J. Grande, C. L. Tang, submitted to *IEEE J. Quantum Electr.* (1992)
9. K. Shigihara, Y. Nagai, S. Karakida, A. Takami, Y. Kokubo, H. Matsubara, S. Kakimoto, *IEEE J. Quantum Electr.*, 27, 1537 (1991).
10. M. Sakamoto, D. F. Welch, G. L. Harnagel, W. Streifer, H. Kung, D. R. Scifres, *Appl. Phys. Lett.* 52, 2220 (1988)
11. W. J. Grande, PhD Dissertation, Cornell University, Ithaca, NY, 14853
12. W. J. Grande, W. D. Braddock, J. R. Sheally, C. L. Tang, *Appl. Phys. Lett.* 51, 2189 (1987)
13. W. J. Grande, J. E. Johnson, C. L. Tang, *J. Vac. Sci. Technol.* B8, 1075 (1990)
14. P. D. Swanson, S. Libby, M. A. Parker, *The Fabrication of Ridge Waveguided Photonic Circuits with Chemically Assisted Ion Beam Etched Mirrors*, USAF Technical Report, 1992 (in preparation)
15. M. A. Parker, A. Olewicz, S. I. Libby, D. Honey, P. D. Swanson, *P⁺ Contacts on GaAs for Semiconductor Lasers*, USAF Technical Report (1992)
16. S. I. Libby, P. D. Swanson, M. A. Parker, *Optical Logic Gate and Component Analysis Techniques*, USAF Technical Report, 1992 (in preparation)
17. S. M. Sze, *Physics of Semiconductor Devices*, 2nd edition, John Wiley and Sons Inc., New York (1981)
18. M. A. Parker, P. D. Swanson, S. I. Libby, *The Importance of Optical Loss for the Differential Efficiency and Threshold Current in Quantum Well Lasers*, Rome Laboratory Technical Memorandum 1992 (in preparation)
19. R. Lang, *Jap. J. Appl. Phys.* 19, L93 (1980)

MISSION
OF
ROME LABORATORY

Rome Laboratory plans and executes an interdisciplinary program in research, development, test, and technology transition in support of Air Force Command, Control, Communications and Intelligence (C3I) activities for all Air Force platforms. It also executes selected acquisition programs in several areas of expertise. Technical and engineering support within areas of competence is provided to ESC Program Offices (POs) and other ESC elements to perform effective acquisition of C3I systems. In addition, Rome Laboratory's technology supports other AFMC Product Divisions, the Air Force user community, and other DOD and non-DOD agencies. Rome Laboratory maintains technical competence and research programs in areas including, but not limited to, communications, command and control, battle management, intelligence information processing, computational sciences and software producibility, wide area surveillance/sensors, signal processing, solid state sciences, photonics, electromagnetic technology, superconductivity, and electronic reliability/maintainability and testability.